WALAILAK JOURNAL
http://wjst.wu.ac.th Applied Mathematics

The Unsteady Flow of a Carreau Fluid Through Inclined Catheterized Arteries Having a Balloon with Time-Variant Overlapping Stenosis

Khaled Saad MEKHEIMER[1,4,*], Faiza SALAMA[2] and Mhamod ELKOT[3]

[1]*Department of Mathematics and Statistics, Faculty of Science, Taif University, Taif, Saudi Arabia*
[2]*Department of Mathematics, Faculty of Science, Suez Canal University, Ismailia, Egypt*
[3]*Department of Mathematics, Faculty of Science, Suez Canal University, Suez, Egypt*
[4]*Department of Mathematics, Faculty of Science, Al-Azhar University, Cairo, Egypt*

([*]Corresponding author's e-mail: kh_mekheimer@yahoo.com)

Received: 10 January 2013, Revised: 22 November 2014, Accepted: 23 December 2014

Abstract

This paper is concerned with the analysis of blood flow through inclined catheterized arteries having a balloon (angioplasty) with time-variant overlapping stenosis. The nature of blood in small arteries are analyzed mathematically by considering it as a Carreau fluid. The analysis is carried out for an artery with a mild stenosis. The problem is formulated using a perturbation expansion in terms of a variant of the Weissenberg number to obtain explicit forms for the axial velocity, the stream function, the pressure gradient, the resistance impedance and the wall shear stress distribution. The results were studied for various values of the physical parameters, such as the Weissenberg number W_i, the power index n, the taper angle ϕ, the maximum height of stenosis δ^*, the angle of inclination α, the maximum height of the balloon σ^*, the axial displacement of the balloon z_d^*, the flow rate F and the Froud number F_r. The results show that the transmission of axial velocity curves through a Newtonian fluid (W_i = 0, n = 1) is substantially lower than that through a Carreau fluid near the wall of the balloon, while the inverse occurs in the region between the balloon and stenosis. The stream lines have a clearly distinguished shifting towards the stenotic region and this shifting appears near the wall of the balloon, while they have almost disappeared near the stenotic wall. Furthermore the size of trapping bolus in the case of the Newtonian fluid (W_i = 0, n = 1) is smaller than that through the Carreau fluid.

Keywords: Carreau fluid, catheterized arterie, overlappings stenosis, unsteady flow, blood flow

Introduction

The study of blood flow through a stenosed artery is very important because the cause and development of many cardiovascular diseases are related to the nature of blood movement and the mechanical behavior of the blood vessel walls. A stenosis is defined as a partial occlusion of the blood vessels due to the accumulation of cholesterol, fats and the abnormal growth of tissue. Cardiac catheterization (also called heart catheterization) is a diagnostic procedure which does a comprehensive examination to determine how the heart and its blood vessels function. One or more catheters can be inserted through a peripheral blood vessel in the arm (antecubital artery or vein) or leg (femoral artery or vein) with X-ray guidance. This procedure gathers information such as adequacy of blood supply through the coronary arteries, blood pressure, blood flow throughout chambers of the heart, collection of blood samples, and X-rays of the heart's ventricles or arteries. The vascular system is injected by a dye to determine any blockages, narrowing, or abnormalities in the coronary arteries. By using X-rays, some visible signs appear which assess in determining the patient's need and his readiness for surgery.

The recent important contributions in that topic are referenced in the literature [1-5]. Much of the research that has studied arteriosclerotic development indicate that the studies are mainly concerned with single symmetric and non-symmetric stenoses while the stenoses may develop in series (multiple stenoses) or may be of irregular shapes or overlapping or composite in nature. Some studies considered an overlapping stenosis in the blood vessel segment. Chakravarty and Mandal [6] noted that the problem becomes more acute in the presence of an overlapping stenosis in the artery instead of a mild one. The effect of vessel tapering is another important factor that was considered. Chakravarty and Mandal [7] formulated the problem on a tapered blood vessel segment having an overlapping stenosis. Ismail *et al*. [8] studied the power-law model of blood flow through an overlapping stenosed artery where an improved shape of the time-variant stenosis in the tapered arterial lumen is given and the vascular wall deformability is taken to be elastic (moving wall). Layek *et al*. [9] investigated the effects of an overlapping stenosis on flow characteristics considering the pressure variation in both the radial and axial directions of the arterial segment under consideration. Srivastava *et al*. [10] addressed the problem of blood flow through an overlapping stenosis assuming that the flowing blood is represented by a two-layered macroscopic two-phase model. Varshney *et al*. [11] studied the effect of overlapping stenosis and externally applied magnetic field on the pulsatile blood flow in arteries where the blood is characterized by a Power-law model. Recently, Mekheimer *et al*. [12] studied the effect of induced magnetic field on blood flow through anisotropically tapered elastic arteries with overlapping of stenosis in an annulus. Morover, Hayat *et al*. [13] discussed the peristaltic flow of a second-order fluid in the presence of an induced magnetic field.

In all the above mentioned studies, horizontal blood carrying vessels were considered. However, it is well-known that many ducts in physiological systems are not horizontal but have some inclination to the axis. The force of gravity arises due to the consideration of inclined arteries. Vajravelu *et al*. [14] studied peristaltic transport of a Herschel-Bulkley fluid in an inclined tube. Maruthi Prasad and Radhakrishnamcharya [15] have proposed steady blood flow through an inclined nonuniform tube with multiple stenoses. Nadeem and Akbar [16,17] discussed the peristaltic transport of Herschel-Bulkley fluid and Walter's B fluid in a non-uniform inclined tube. Prasad *et al*. [18] studied the peristaltic transport of micropolar fluid in an inclined tube under the assumptions of long wavelength and low Reynolds number. Recently, Chakraborty *et al*. [19] studied the effects of slip condition (at the stenotic wall), hematocrit and inclination of the artery on the flow variables (wall shear stress, shear stress at the throat of the stenosis and resistance to the flow) for blood flow through an inclined vessel with an axially non-symmetric mild stenosis, taking into account that blood which is represented by a particle-fluid suspension. Most of these studies do not study the effect of the catheter that have a balloon (angioplasty) on blood flow through inclined artery with overlapped stenosis which occurs in many clinical applications.

For the flows of non-Newtonian fluids there is not a single model that describes all of their properties as there is for the Newtonian fluid. The flows of such fluids can be analyzed with the help of a power-law model. However, now in addition to the viscosity, another parameter, namely the power-law index (or exponent) is used to characterize the flows of such fluids that can be analyzed with the help of a power-law model [20]. Ellahi *et al*. [21] discussed the peristalic flow of Carreau fluid in a rectangular duct through a porous medium.

In this paper, our primary concern is the four parameter model that does not have a discontinuous first derivative is a Carreau model. The Carreau fluid reveals (shear-thinning) that the viscosity decreases with increasing shear rate, by reaching 10^{-3} or 10^{-4} for a zero-shear rate. This factor is often the most important property for engineering calculations [23].

With the above discussion in mind, the goal of this investigation is to study the effect of the catheter that have a balloon (angioplasty) on the flow of the Carreau fluid (as a blood model) through inclined arteries with time-variant overlapped stenosis. The problem is first modeled and then the non-dimensional governing equations in the case of mild stenosis with the corresponding boundary conditions are prescribed and solved analytically. The results for the resistance impedance, wall shear stress distribution, the axial velocity, the pressure gradient have been discussed for various values of the problem parameters. Also the contour plots for the stream function are discussed. Finally, the main findings of the results are summarized as concluding remarks.

Mathematical model

Consider an incompressible Carreau fluid of viscosity μ and density ρ flowing through coaxial tubes such that the inner tube represents the catheter with a balloon (angioplasty) on its wall and assuming that the balloon model is axi-symmetric in nature while the outer tube has a finite length L with overlapping stenosis and inclined at an angle α to the horizontal. Let (r,θ,z) be the coordinates of a material point in the cylindrical polar coordinate system where the z - axis is taken along the axis of the artery while r, θ are along the radial and circumferential directions respectively. Further, we assume that $r=0$ is taken as the axis of symmetry of the coaxial tubes. The geometry of the arterial wall with time-variant overlapping stenosis and the balloon model are defined by the functions $R(z,t)$ and $h(z)$, respectively, as shown as in **Figure 1**, and can be written mathematically as [8,23];

$$R(z,t) = [(mz+R_o) - \frac{\delta\cos\phi}{L_o}(z-d)\{11 - \frac{94}{3L_o}(z-d) + \frac{32}{L_o^2}(z-d)^2$$
$$-\frac{32}{3L_o^3}(z-d)^3\}]\Omega(t) \qquad d \le z \le d+\frac{3L_o}{2}$$
$$= (mz+R_o)\Omega(t) \qquad otherwise \tag{1}$$

The time-variant parameter $\Omega(t)$ is taken to be;

$$\Omega(t) = 1-\varepsilon(\cos\omega t - 1)\exp[-\varepsilon\omega t], \tag{2}$$

$$h(z) = R_o[k+\sigma\exp-\pi^2(z-z_d-0.5)^2] \qquad d \le z \le d+\frac{3L_o}{2}$$
$$= kR_o \qquad otherwise \tag{3}$$

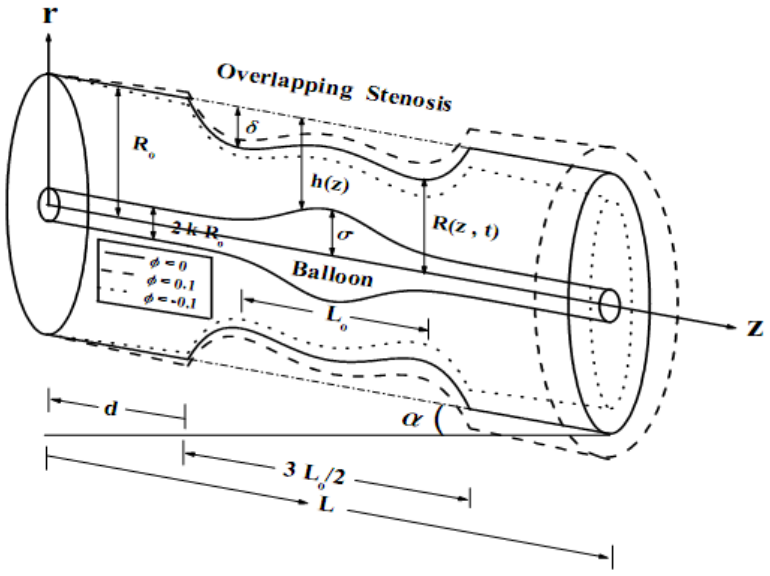

Figure 1 Schematic diagram of a catheterized overlapping stenosed artery.

where R_o is the constant radius of the normal artery in the non-stenotic region, ϕ is the angle of tapering, $\frac{3L_o}{2}$ is the length of the overlapping stenosis, d is the location of the stenosis, $\delta\cos\phi$ is taken to be the critical height of the overlapping stenosis, $m = (\tan\phi)$ represents the slope of the tapered vessel, ε is a constant, ω represents the angular frequency of the forced oscillation and t is the time, σ denotes the maximum height attained by the balloon at $(z = z_d + 0.5)$, k R_o is the radius of the inner tube which keeps the balloon in position, $k << 1$ and z_d represents the axial displacement of the balloon. We can explore the possibility of different shapes of the artery viz, the converging tapering ($\phi < 0$), non-tapered artery ($\phi = 0$) and the diverging tapering ($\phi > 0$) [24].

The equations governing unsteady flow of an incompressible Carreau fluid are;

$$\frac{\partial V_r}{\partial r} + \frac{V_r}{r} + \frac{\partial V_z}{\partial z} = 0, \tag{4}$$

$$\rho\left(\frac{\partial}{\partial t} + V_r\frac{\partial}{\partial r} + V_z\frac{\partial}{\partial z}\right)V_r = -\frac{\partial p}{\partial r} + \frac{1}{r}\frac{\partial}{\partial r}(r\tau_{rr}) + \frac{\partial}{\partial z}(\tau_{rz}) - \frac{\tau_{\theta\theta}}{r} - \rho g\cos(\alpha), \tag{5}$$

$$\rho\left(\frac{\partial}{\partial t} + V_r\frac{\partial}{\partial r} + V_z\frac{\partial}{\partial z}\right)V_z = -\frac{\partial p}{\partial z} + \frac{1}{r}\frac{\partial}{\partial r}(r\tau_{rz}) + \frac{\partial}{\partial z}(\tau_{zz}) + \rho g\sin(\alpha), \tag{6}$$

where p is the fluid pressure, V_r and V_z are the velocity components in radial and axial directions respectively, g is the acceleration due to gravity and α is the angle of inclination.

The extra stress tensor for a Carreau fluid is defined by [22];

$$\tau_{ij} = [\eta_\infty + (\eta_o - \eta_\infty)(1 + (\Gamma\dot{\gamma})^2)^{\frac{n-1}{2}}]\dot{\gamma}_{ij}, \tag{7}$$

where τ_{ij}, $i, j = r, \theta, z$ are the components of the extra stress tensor, η_∞ is the infinite shear rate viscosity, η_o is the zero shear rate viscosity, Γ is a time constant, n is the dimensionless power law index and $\dot{\gamma}$ is defined as;

$$\dot{\gamma} = \sqrt{\frac{1}{2}\sum_i\sum_j \dot{\gamma}_{ij}\dot{\gamma}_{ij}} = \sqrt{\frac{1}{2}\prod_{\dot{\gamma}_{ij}}}, \tag{8}$$

where $\prod$ is the second invariant of the strain rate tensor $\dot{\gamma}_{ij}$. According to Bird *et al*. [25] and Tanner [26], we consider in the constitutive Eq. (7) the case for which η_∞ = 0, and $\Gamma\dot{\gamma} << 1$ [15]. So we can write the components of extra stress tensor as;

$$\tau_{ij} = \eta_o[1 + \frac{n-1}{2}\Gamma^2\dot{\gamma}^2]\dot{\gamma}_{ij}. \tag{9}$$

The boundary conditions are;

$$V_r = 0, \quad V_z = 0 \quad at \quad r = h(z) \quad and \quad r = R(z,t). \tag{10}$$

We introduce the following non-dimensional variables;

$$r = R_o r', \quad z = L_o z', \quad V_r = \frac{\delta u_o}{L_o}V_r', \quad V_z = u_o V_z', \quad \tau_{ij} = \frac{u_o\eta_o}{R_o}\tau_{ij}', \quad \dot{\gamma} = \frac{u_o}{R_o}\dot{\gamma}',$$

$$\dot{\gamma}_{ij} = \frac{u_o}{R_o}\dot{\gamma}_{ij}', \quad h = R_o h', \quad R = R_o R', \quad \omega = \frac{u_o\omega'}{L_o}, \quad t = \frac{L_o}{u_o}t', \quad p = \frac{u_o L_o \mu}{R_o^2}p',$$

$$W_i = \frac{u_o\Gamma}{R_o}, \quad R_e = \frac{\rho u_o R_o}{\mu}, \quad E = \frac{F_r}{R_e}, \quad F_r = \frac{u_o^2}{gR_o}. \tag{11}$$

where W_i is the Weissenberg number, R_e is the Reynolds number, $E = \frac{F_r}{R_e}$ is a dimensionless quantity, F_r is the Froud number and u_o is the velocity averaged over the section of the tube with a radius R_o.

We non-dimensionalize Eqs. (4) - (9) by using Eq. (11) to find the appropriate equations describing the flow of a Carreau fluid in the case of a mild stenosis $(\delta^* = \frac{\delta}{R_o} << 1)$, subject to the additional condition $(\frac{R_o}{L_o} \simeq o(1))$ [27] after dropping the dashes as;

$$\frac{\partial p}{\partial r} = 0, \tag{12}$$

$$\frac{\partial p}{\partial z} = \frac{1}{r}\frac{\partial}{\partial r}[r(\frac{\partial V_z}{\partial r} + \frac{(n-1)W_i^2}{2}(\frac{\partial V_z}{\partial r})^3)] + \frac{\sin(\alpha)R_e}{F_r}. \tag{13}$$

The corresponding boundary conditions (dropping dashes) are;

$$V_z = 0 \qquad at \quad r = h(z) \quad and \quad r = R(z,t), \tag{14}$$

with

$$R(z,t) = [(m^* z + 1) - \delta^* \cos\phi(z - d^*)\{11 - \frac{94}{3}(z - d^*) + 32(z - d^*)^2$$

$$-\frac{32}{3}(z - d^*)^3\}]\Omega(t) \qquad d^* \le z \le d^* + \frac{3}{2} \tag{15}$$

$$= (m^* z + 1)\Omega(t) \qquad otherwise,$$

and

$$h(z) = k + \sigma^* \exp[-\pi^2(z - z_d^* - 0.5)^2] \qquad d^* \le z \le d^* + \frac{3}{2} \tag{16}$$

$$= k \qquad otherwise,$$

where $m^* = \frac{L_o m}{R_o}$, $d^* = \frac{d}{L_o}, \sigma^* = \sigma \exp[L_o^2]$ and $z_d^* = \frac{z_d + 0.5(1 - L_o)}{L_o}$.

Solution development

We expand the dependent variables as follows;

$$V_z = V_{zo} + W_i^2 V_{z1} + O(W_i^4),$$
$$p = p_o + W_i^2 p_1 + O(W_i^4),$$
$$F = F_o + W_i^2 F_1 + O(W_i^4). \tag{17}$$

After some straight forward calculations the solutions of the axial velocity and the pressure gradient together with the corresponding boundary conditions will be in the forms;

$$V_z(r,z,t)=\frac{1}{4}\left(\frac{dp}{dz}-\frac{\sin(\alpha)R_e}{F_r}\right)\{r^2-R^2+S\log\left(\frac{r}{R}\right)\}$$
$$-\frac{(n-1)W_i^2\left(\frac{dp_o}{dz}-\frac{\sin(\alpha)R_e}{F_r}\right)^3}{128}\{2(r^2-R^2)(r^2+R^2+3S+\frac{S^3}{4r^2R^2})$$
$$+(6S^2+2S(h^2+R^2)+\frac{S^4}{2h^2R^2})\log\left(\frac{r}{R}\right)\}, \tag{18}$$

$$\frac{dp}{dz}=\left(\frac{-16F}{\Phi}\right)+\frac{\sin(\alpha)R_e}{F_r}-\frac{(n-1)W_i^2\beta\left(\frac{dp_o}{dz}-\frac{\sin(\alpha)R_e}{F_r}\right)^3}{8\Phi}, \tag{19}$$

where

$$S=\frac{(h^2-R^2)}{\log\left(\frac{R}{h}\right)},\quad \Phi=(R^2-h^2)(R^2+h^2+S)$$

$$\beta=\frac{(R^6-h^6)}{3}+\frac{3S(R^4-h^4)}{2}+\left(\frac{S^3}{4R^2}-3SR^2-R^4\right)(R^2-h^2)-\frac{S^3}{2}\log\left(\frac{R}{h}\right)$$

$$+\frac{1}{4}(6S^2+2S(h^2+R^2)+\frac{S^4}{2h^2R^2})(h^2-R^2-2h^2\log\left(\frac{h}{R}\right)). \tag{20}$$

The corresponding stream function ($V_z=\frac{1}{r}\frac{\partial\psi}{\partial r}$ with $\psi=0$ at $r=h$) is;

$$\psi(r,z,t)=\frac{1}{4}\left(\frac{dp}{dz}-\frac{\sin(\alpha)R_e}{F_r}\right)\{\frac{(r^2-h^2)(r^2+h^2-2R^2-S)}{4}+\frac{S}{2}(r^2\log\left(\frac{r}{R}\right)$$
$$-h^2\log\left(\frac{h}{R}\right))\}-\frac{(n-1)W_i^2\left(\frac{dp_o}{dz}-\frac{\sin(\alpha)R_e}{F_r}\right)^3}{128}\{\frac{(r^6-h^6)}{3}+\frac{3S(r^4-h^4)}{2}$$
$$+\frac{1}{4}(r^2-h^2)(\frac{S^4}{2h^2R^2}+\frac{S^3}{R^4}+6S^2+2S(h^2-5R^2)-4R^4)-\frac{S^3\log\left(\frac{r}{h}\right)}{2}$$
$$+\frac{1}{2}(\frac{S^4}{2h^2R^2}+6S^2+2S(h^2+R^2))(r^2\log\left(\frac{r}{R}\right)-h^2\log\left(\frac{h}{R}\right))\} \tag{21}$$

Using Eq. (18), we can find the expression for the wall shear stress in the form;

$$\tau_{rz} = (\frac{\partial V_z}{\partial r} + \frac{(n-1)W_i^2}{2}(\frac{\partial V_z}{\partial r})^3)\,|_{r=R(z,t)}\,. \tag{22}$$

Since the flow rate F is constant for all the sections of the tube, the pressure drop across the length of the overlapping stenosis is;

$$\Delta p = \int_0^{L^*}(-\frac{dp}{dz})dz = F\int_0^{L^*}\chi(z,t)dz. \tag{23}$$

where

$$\chi(z,t) = (\frac{16}{\Phi}) - \frac{\sin(\alpha)R_e}{FF_r} + \frac{(n-1)W_i^2\beta(\frac{dp_o}{dz} - \frac{\sin(\alpha)R_e}{F_r})^3}{8\Phi F}. \tag{24}$$

The resistance to flow (resistance impedance) experienced by the flowing blood in the arterial segment under consideration using Eq. (24) may be defined as;

$$\lambda = \frac{\Delta p}{F}$$
$$= [\int_0^{d^*}\Sigma(z,t)dz + \int_{d^*}^{d^*+\frac{3}{2}}\chi(z,t)dz + \int_{d^*+\frac{3}{2}}^{L^*}\Sigma(z,t)dz]. \tag{25}$$

where $\Sigma(z,t) = \chi(z,t)\,|_{R=(m^*z+1)\Omega(t)\quad and\quad h=k}$.

Graphical results and discussion

Computer codes are developed to evaluate the analytic results obtained for the axial velocity V_z, the resistance impedance λ and the wall shear stress distribution τ_{rz} in order to be able to discuss the results obtained in Eqs. (18), (23) and (25) quantitatively, we use the following experimental data [8]: $\varepsilon = 0.1,\quad L_o = 1,\quad d^* = 0.75,\quad \omega = 7.854\quad and\quad R_e = 1.$

According to Bird *et al*. [25] and Tanner [26] the Carreau fluid parameters are $n = 0.398, 0.496$ and $\Gamma = 1.04, 1.58$. The Weissenberg number physically means that the viscosity decreases as W_i increases and it is directly proportional to the relaxation time with constant averaged velocity over the section of the tube and the radius of the tube. When $(n = 1\ ,\ W_i = 0)$ the fluid will become a Newtonian one.

Figures 2a and **2b** describe the distribution of the axial velocity V_z for different values of the Weissenberg number W_i and power low index n; we prepared **Figures 2a** and **2b** for various values of the parameters: $t = 0.5$, $z = 1.2$, $\delta^* = 0.1$, $\sigma^* = 0.2$, $\phi = 0$, $F = 0.7$, $\alpha = 15^o$, $F_r = 0.1$,

$z_d^* = 1,\ \frac{dp_o}{dz} = 1.5,\ k = 0.01,\ (n = 0.398,\ W_i = 0, 0.4, 0.8),\ (W_i = 0.5,\ n = 0.398, 0.496, 1).$

It is observed that the axial velocity increases by increasing the Weissenberg number W_i while it decreases by increasing the power low index n in the region ($0.09 \le r \le 0.43$) (near the wall of the balloon) and opposite behavior occurs in the region ($0.43 \le r \le 0.9$, the region between the balloon and stenosis). Also we can record that the axial velocity is approximately independent of W_i and n in the region ($0.9 \le r \le 1.07$) (near the wall of stenosis) for both Newtonian and non-Newtonian fluids. Hence we can say that the transmission of the axial velocity curves through a Newtonian fluid ($W_i = 0, n = 1$) is substantially lower than that through a Carreau fluid in the region near the wall of the balloon while the inverse occurs in the region between the balloon and stenosis.

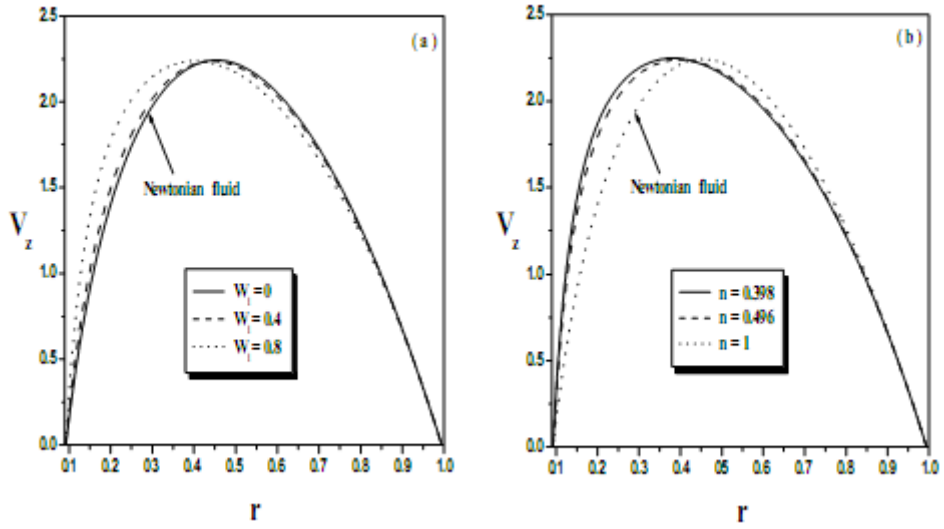

Figure 2 Variation of velocity profiles V_z with r for different values of the Weissenberg number W_i and power low index n (panels (a) and (b) respectively).

Figures 3a and **3b** show the variation of the axial velocity V_z with radial distance r for different values of the taper angle ϕ and the flow rate F. To see the effect of ϕ and F on the axial velocity, we prepared **Figures 3a** and **3b** for various values of the parameters: $t = 0.5,\ z = 1.2,\ \delta^* = 0.1,\ \sigma^* = 0.2,\ W_i = 0.1,\ n = 0.398,\ \alpha = 15^o,\ F_r = 0.1,\ z_d^* = 1,\ \frac{dp_o}{dz} = 1.5,\ k = 0.01,\ (F = 0.3,\ \phi = 0, 0.05, -0.05),\ (\phi = 0,\ F = 0.3, 0.6, 0.9)$. The effect of the vessel tapering together with the shape of stenosis on the blood flow characteristics seem to be equally important and hence deserve special attention. The tapering is a significant aspect of the mammalian arterial system, and it is interested in the flow through a tapered artery with stenosis. So we can see that the curves through the converging tapered artery $\phi = -0.05$ (< 0) are higher than those in the non-tapered artery $(\phi = 0)$ and the diverging tapered artery $\phi = 0.05$ (> 0) in the region ($0.09 \le r \le 0.78$) while the inverse occurs in

the region ($0.78 \le r \le 1.07$). Furthermore it is indicated from these figures that the magnitude of the axial velocity increases by increasing the flow rate F .

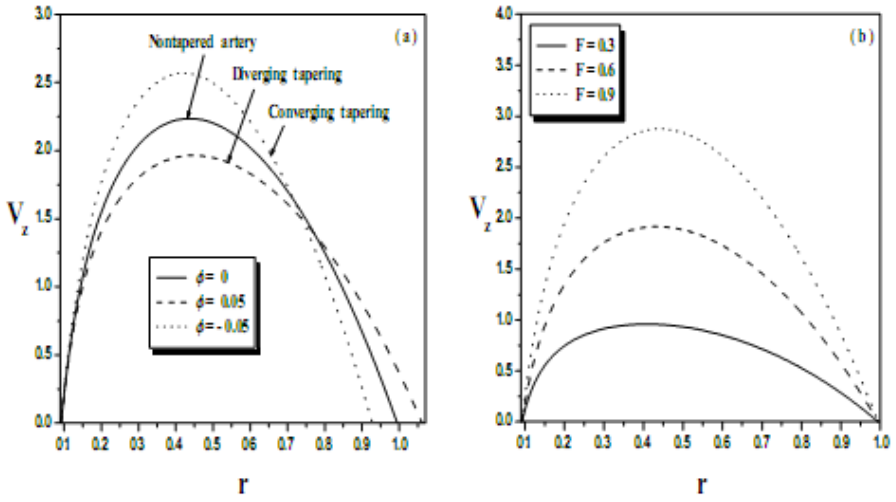

Figure 3 Variation of velocity profiles V_z with r for different values of the taper angle ϕ and flow rate F (panels (a) and (b) respectively).

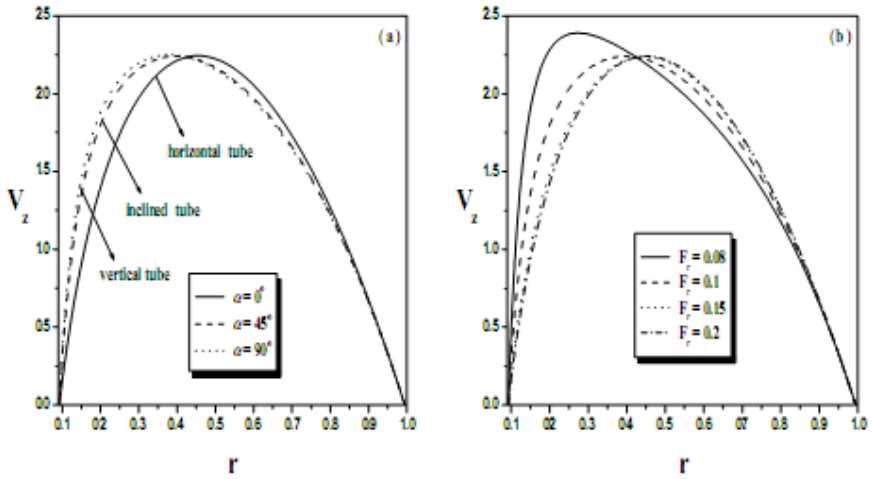

Figure 4 Variation of velocity profiles V_z with r for different values of the angle of inclination α and Froud number F_r (panels (a) and (b) respectively).

The effects of the angle of inclination α and Froud number F_r on the axial velocity V_z are displayed in **Figures 4a** and **4b**. To discuss these effects we use the following data: $t = 0.5$, $z = 1.2$, $\delta^* = 0.1$, $\sigma^* = 0.2$, $W_i = 0.5$, $n = 0.398$, $\phi = 0$, $F = 0.7$, $z_d^* = 1$, $\frac{dp_o}{dz} = 1.5$, $k = 0.01$, ($F_r = 0.1$, $\alpha = 0^o, 45^o, 90^o$), ($\alpha = 45^o$, $F_r = 0.08, 0.1, 0.15, 0.2$). It is noted that the axial velocity increases by increasing the angle of inclination α while it decreases by increasing the Froud number F_r in the region ($0.09 \le r \le 0.43$) and the opposite behavior occurs in the region ($0.43 \le r \le 0.9$); also the axial velocity is independent of α and F_r in the region ($0.9 \le r \le 1.07$). The magnitude of the axial velocity clearly increases by increasing the acceleration due to the gravity g near the wall of the balloon at small values of the Froud number F_r while by increasing the values of the Froud number F_r gradually, the effect of gravity on the axial velocity is very negligible. The magnitude of the axial velocity through the vertical tube $(\alpha = 90^o)$ is higher than those in the inclined tube $(\alpha = 45^o)$ and the horizontal tube $(\alpha = 0^o)$ near the wall of the balloon while the inverse occurs in the region between the balloon and stenosis.

The wall shear stress is important in understanding the development of arterial disease because of the strong correlation between the localization of arteriosclerosis (stenosis) and the arterial wall. The variation of the wall shear stress distribution τ_{rz} in the stenotic region $(0.75 \le z \le 2.25)$ for different values of the maximum height of stenosis δ^* and the maximum height of the balloon σ^* is shown in **Figures 5a** and **5b**, for various values of the parameters: $t = 0.5$, $\alpha = 45^o$, $F_r = 0.1$, $W_i = 0.1$, $n = 0.398$, $\phi = 0$, $F = 0.3$, $z_d^* = 1$, $\frac{dp_o}{dz} = 1.5$, $k = 0.05$, ($\sigma^* = 0.01$, $\delta^* = 0.05, 0.1, 0.15$), ($\delta^* = 0.01$, $F_r = 0.1, 0.2, 0.3$). It is observed that the wall shear stress distribution curves are linear for $\sigma^* = 0.0$, $\delta^* = 0.0$ (no stenosis or a ballon) and non-linear for $\sigma^* \neq = 0.0$, $\delta^* \neq 0.0$, also from these figures τ_{rz} decreases by increasing the maximum height of stenosis δ^* and the maximum height of the balloon σ^*. Hence, the magnitude of the wall shear stress distribution is higher in the case of no-stenosis ($\delta^* = 0$) (uniform tube) than that for the stenosis.

The variation of the wall shear stress distribution τ_{rz} in the stenotic region for different values of axial displacement of the balloon z_d^* and taper angle ϕ is displayed in **Figures 6a** and **6b**. By using the following data: $t = 0.5$, $\alpha = 45^o$, $F_r = 0.1$, $W_i = 0.1$, $n = 0.398$, $\delta^* = 0.1$, $F = 0.3$, $\sigma^* = 0.2$, $\frac{dp_o}{dz} = 1.5$, $k = 0.05$, ($\phi = 0$, $z_d^* = 0, 0.2, 0.4$), ($z_d^* = 1, \phi = 0, 0.05, -0.05$), we can record that by increasing the axial displacement of the balloon z_d^*, the curves have shifted towards the left and the magnitude of the wall shear stress distribution decreases, and this effect decays as we move away from the balloon. It is also observed that the curves through the diverging tapered artery $\phi = 0.05$ (> 0) are higher than those in the non-tapered artery $(\phi = 0)$ and the converging tapered artery $\phi = -0.05$ (< 0).

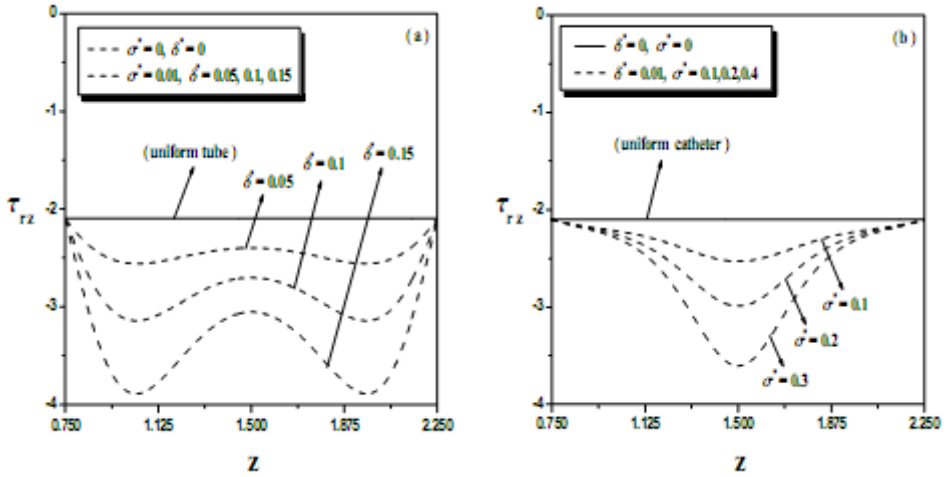

Figure 5 Variation of the wall shear stress distribusion τ_{rz} with z for different values of maximum height of stenosis δ^* and maximum height of balloon σ^* (panels (a) and (b) respectively).

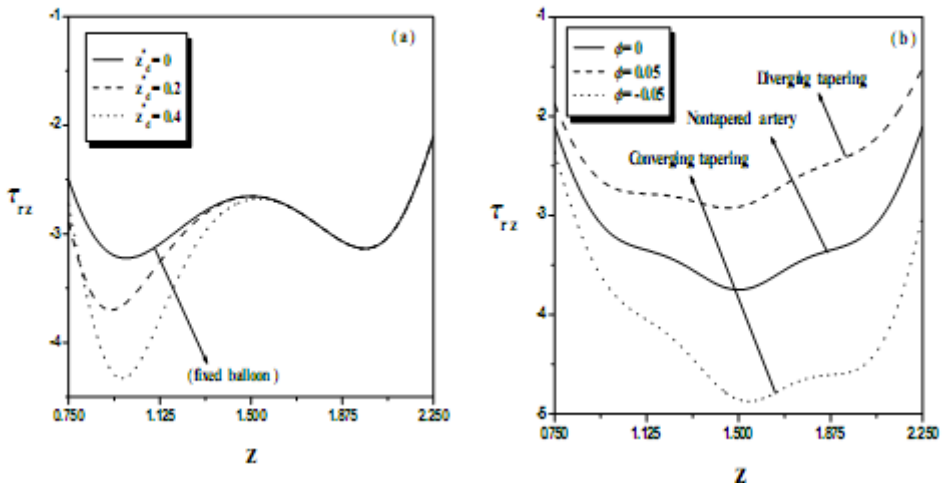

Figure 6 Variation of the wall shear stress distribusion τ_{rz} with z for different values of axial displasement of the balloon z_d^* and taper angle ϕ (panels (a) and (b) respectively).

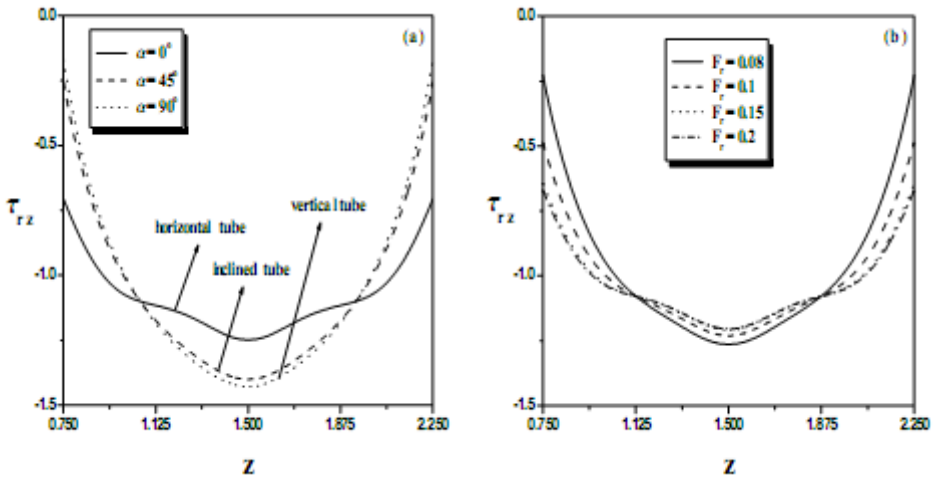

Figure 7 Variation of the wall shear stress distribusion τ_{rz} with z for different values of angle of inclination α and Froud number F_r (panels (a) and (b) respectively).

Figures 7a and **7b** illustrate the variation of the wall shear stress distribution τ_{rz} in the stenotic region for different values of the angle of inclination α and Froud number F_r, with the data: $t = 0.5$, $\phi = 0$, $z_d^* = 1$, $W_i = 0.3$, $n = 0.398$, $\delta^* = 0.1$, $F = 0.1$, $\sigma^* = 0.2$, $\frac{dp_o}{dz} = 1.5$, $k = 0.03$, ($F_r = 0.08$, $\alpha = 0^o, 45^o, 90^o$), ($\alpha = 15^o$, $F_r = 0.08, 0.1, 0.15, 0.2$). These figures show that the wall shear stress distribution decreases by increasing the angle of inclination α while it increases by increasing the Froud number F_r in the region ($1.05 \le z \le 1.93$) and the opposite behavior occurs in the regions ($0.75 \le z \le 1.05$) and ($1.93 \le z \le 2.25$). Also the curves through the horizontal tube ($\alpha = 0^o$) are higher than those in the inclined tube ($\alpha = 45^o$) and the vertical one ($\alpha = 90^o$) in the region ($1.05 \le z \le 1.93$) and the inverse occurs in the regions ($0.75 \le z \le 1.05$) and ($1.93 \le z \le 2.25$).

The variation of the wall shear stress distribution τ_{rz} in the stenotic region for different values of the Weissenberg number W_i and power low index n is displayed in **Figures 8a** and **8b** by using the following data: $t = 0.5$, $\alpha = 45^o$, $F_r = 0.1$, $\phi = 0$, $\delta^* = 0.1$, $F = 0.3$, $\sigma^* = 0.2$, $\frac{dp_o}{dz} = 1.5$, $k = 0.01$, ($n = 0.398$, $W_i = 0, 0.1, 0.2$), ($W_i = 0.3$, $n = 0.398, 0.496, 1$). It is observed that wall shear stress distribution increases by increasing the Weissenberg number W_i while it decreases by increasing the power low index n and the transmission of the wall shear stress curves through a Newtonian fluid ($W_i = 0, n = 1$) is substantially higher than that through a Carreau fluid.

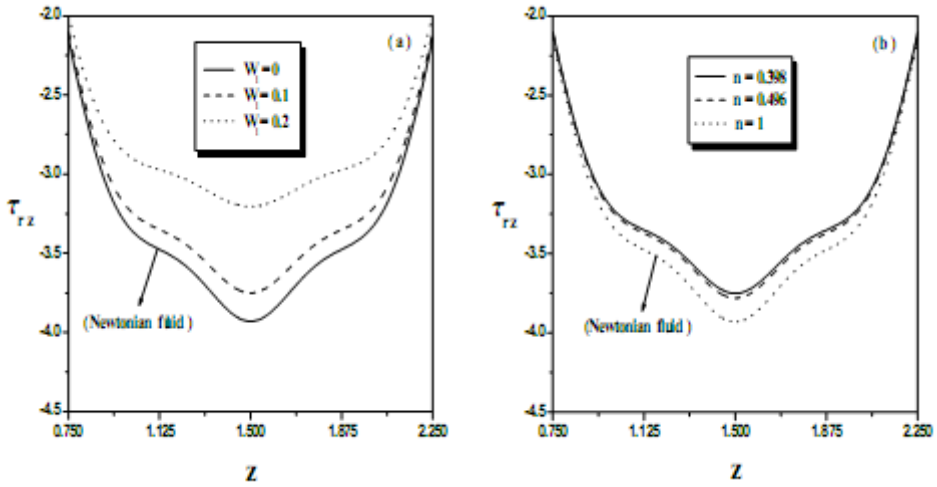

Figure 8 Variation of the wall shear stress distribusion τ_{rz} with z for different values of the Weissenberg number W_i and power low index n (panels (a) and (b) respectively).

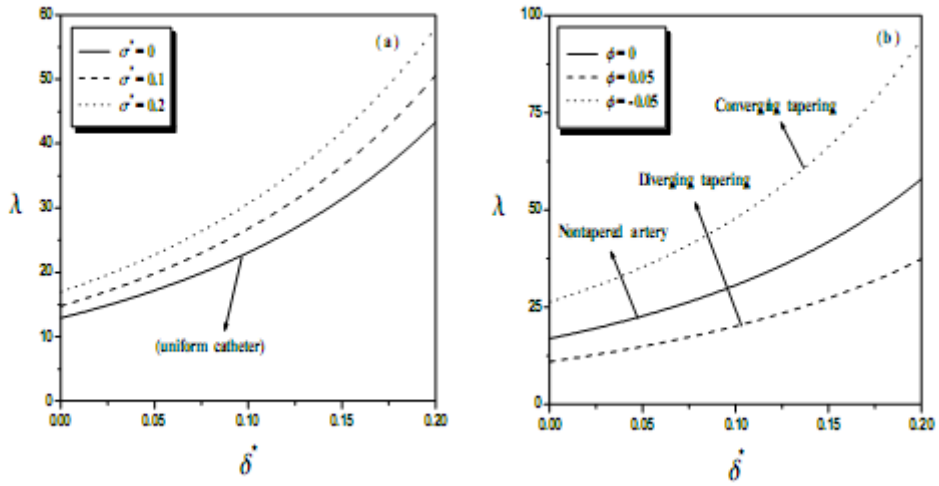

Figure 9 Variation of resistance impedance (resistance to flow) λ with δ^* for different values of the maximum height of the balloon σ^* and taper angle ϕ (panels (a) and (b) respectively).

Figures 9a and **9b** illustrate the variation of the resistance to flow λ (resistance impedance) with the maximum height of stenosis δ^* for different values of the maximum height of the balloon σ^* and taper angle ϕ. To see the effects of σ^* and ϕ on resistance impedance, we prepared these figures with the data: $t = 0.5$, $\alpha = 15^o$, $F_r = 0.1$, $n = 0.398$, $F = 0.1$, $W_i = 0.1$, $\frac{dp_o}{dz} = 1.5$, $k = 0.01$,

$L^* = 3$, $z_d^* = 1$, ($\phi = 0$, $\sigma^* = 0, 0.1, 0.2$), ($\sigma^* = 0.3$, $\phi = 0, 0.05, -0.05$). It is observed that the resistance impedance increases by increasing σ^* and the magnitude of the resistance impedance is higher in the case of a catheter with a balloon ($\sigma^* \neq 0$) than that for the case of a uniform catheter ($\sigma^* = 0$) also the λ curves through the converging tapered artery $\phi = -0.05$ (< 0) are higher than those in the non-tapered artery ($\phi = 0$) and diverging tapered artery $\phi = 0.05$ (> 0).

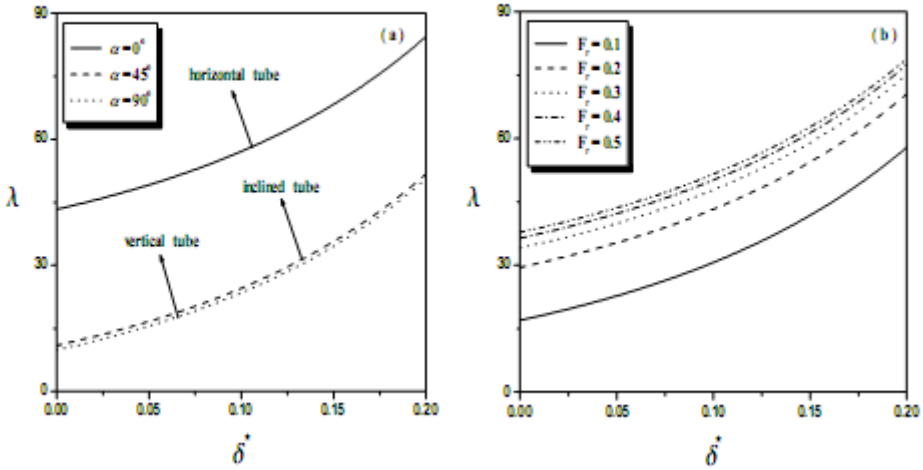

Figure 10 Variation of resistance impedance (resistance to flow) λ with δ^* for different values of the angle of inclination α and Froud number F_r (panels (a) and (b) respectively).

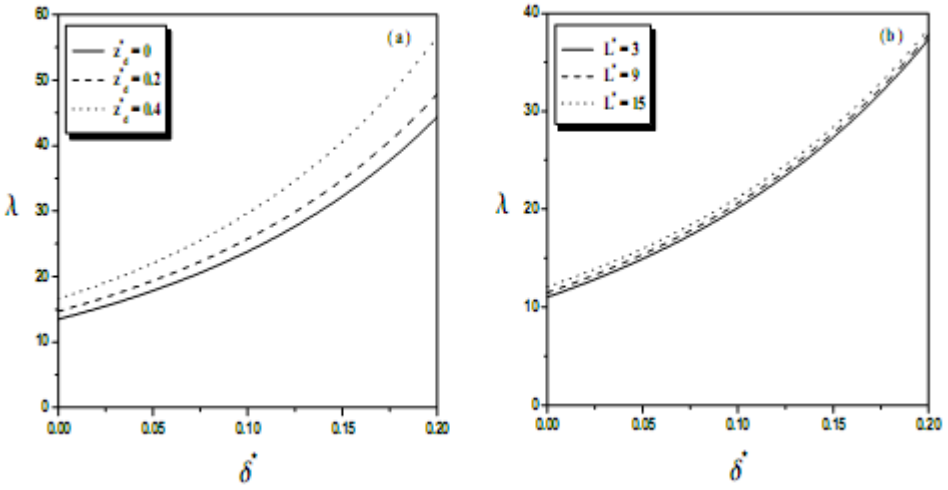

Figure 11 Variation of resistance impedance (resistance to flow) λ with δ^* for different values of the axial displasement of the balloon z_d^* and length of the artery L^* (panels (a) and (b) respectively).

The variations of the resistance to flow (resistance impedance) λ with δ^* for different values of the angle of inclination α, Froud number F_r, the axial displacement of the balloon z_d^* and the length of the artery L^* are displayed in **Figures 10** and **11** for various values of the parameters: $t = 0.5$, $\phi = 0$, $n = 0.398$, $F = 0.7$, $W_i = 0.1$, $\frac{dp_o}{dz} = 1.5$, $k = 0.01$, $\sigma^* = 0.2$, $(\alpha = 0^o, 45^o, 90^o)$, $(F_r = 0.1, 0.2, 0.3, 0.4, 0.5)$, $(z_d^* = 0, 0.2, 0.4)$ and $(L^* = 3, 9, 15)$. It is observed that the resistance impedance decreases by increasing the angle of inclination α, for $\alpha > 45^o$ this variation takes a constant value and there is no effect of α on the the resistance to flow λ. These results agree closely with those of Vajravelu *et al*. [14], Nadeem and Akbar [16] and Chakraborty *et al*. [19]. Also, the magnitude of resistance impedance λ increases by increasing both z_d^* and L^*, where a small variation in the length of the artery L^* on λ is observed. The magnitude of resistance impedance increases by increasing the Froud number F_r, i.e, it decreases as the acceleration due to gravity g increases and as the values of the Froud number F_r increases gradually, the effect of gravity on resistance impedance λ is very small. Hence, the magnitude of resistance impedance through a horizontal tube $(\alpha = 0^o)$ is higher than those in the inclined tube $(\alpha = 45^o)$ and vertical one $(\alpha = 90^o)$ and there is no variation for $(\alpha > 45^o)$.

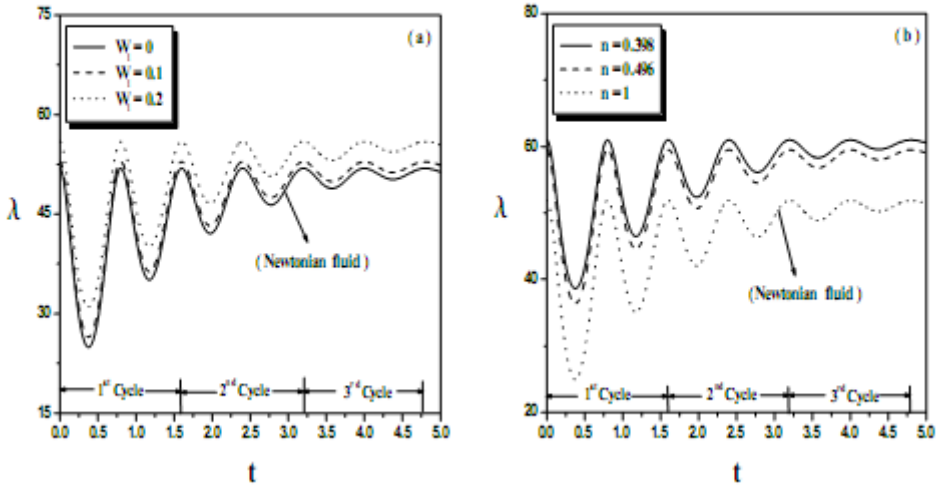

Figure 12 Variation of resistance impedance (resistance to flow) λ with t for different values of the Weissenberg number W_i and power low index n (panels (a) and (b) respectively).

It is clear that the resistance impedance profiles with the time t have a periodic oscillation form and there are three cardiac cycles where the length of the cycle is equal to 1.6 approximately (see **Figures 12a** and **12b**). In the first cycle, the magnitude of the resistance impedance starts decreasing to reach its minimum value then starts increasing to reach its maximum then repeats its form again to reach the

beginning point of the second cycle and so on. Also we can see that the magnitude of the resistance impedance take similar variations in the second and third cycles. Moreover, this oscillation decays as the time t increases. We can record that the resistance impedance increases by increasing W_i and n. So, the transmission of the resistance impedance curves through a Carreau fluid is substantially higher than that through a Newtonian fluid ($W_i = 0, n = 1$).

Trapping represents an interesting phenomenon for the fluid flow, where the streamlines under certain conditions split to trap a bolus which moves as a whole with the fluid. The formation of an internally circulating bolus of the fluid by closed streamline is called trapping. The bolus defined as a volume of fluid bounded by closed streamlines. **Figures 13 - 17** represent the graphical behavior for this phenomena. **Figure 13** reveals that the size of trapping bolus decreases by increasing the axial displacement of the balloon z_d^* and the streamlines have clearly distinguished shifting toward the stenotic region $(0.75 \le z \le 2.25)$ also at ($z_d^* = 1$), the balloon keeps its position in the stenotic region. This shifting appears near the wall of the balloon, while it disappeared near the stenotic wall.

We can record that the size of the trapped bolus increases clearly by increasing the maximum height of the balloon σ^* (**Figure 14**). **Figure 15** indicates that the size of the trapped bolus through the vertical tube $(\alpha = 90^o)$ is higher than that in the inclined tube $(\alpha = 45^o)$ and the horizontal one $(\alpha = 0^o)$. The effects of the Weissenberg number W_i and power low index n on the trapping are displayed in **Figures 16** and **17**. It is observed that the trapping appears near the overlapping stenosis wall and the trapped bolus increases in size as the Weissenberg number W_i while it decreases in size by increasing the power low index n. Finally we can see the size of the bolus in the case of a Newtonian fluid ($W_i = 0, n = 1$) is smaller than that for a Carreau fluid.

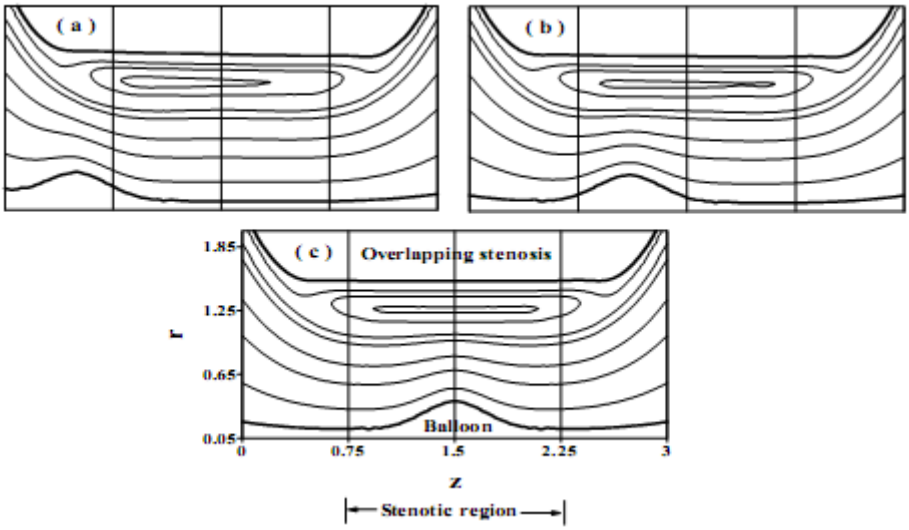

Figure 13 Plot showing streamlines for different values of axial displasement of the balloon with (a) z_d^* = 0, (b) z_d^* = 0.6 and (c) z_d^* = 1.

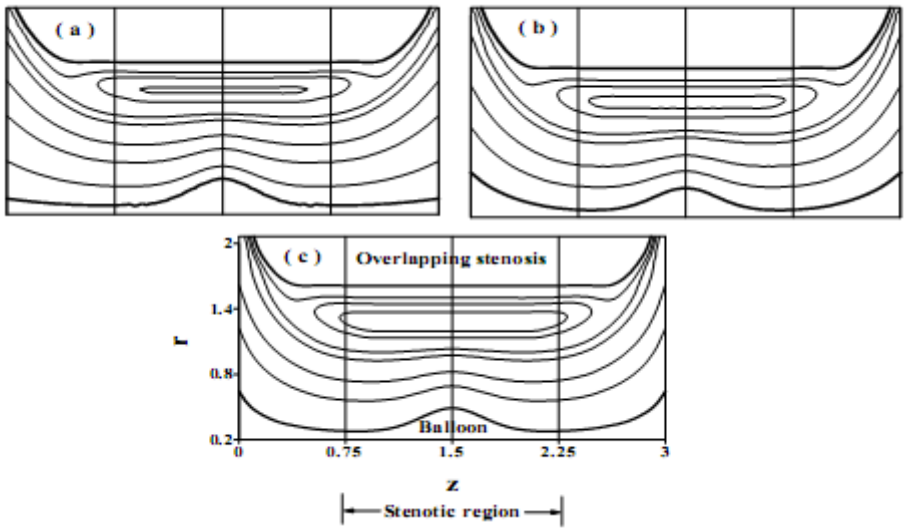

Figure 14 Streamlines for different values of the maximum height of the balloon with (a) σ^* = 0.3, (b) σ^* = 0.4 and (c) σ^* = 0.5.

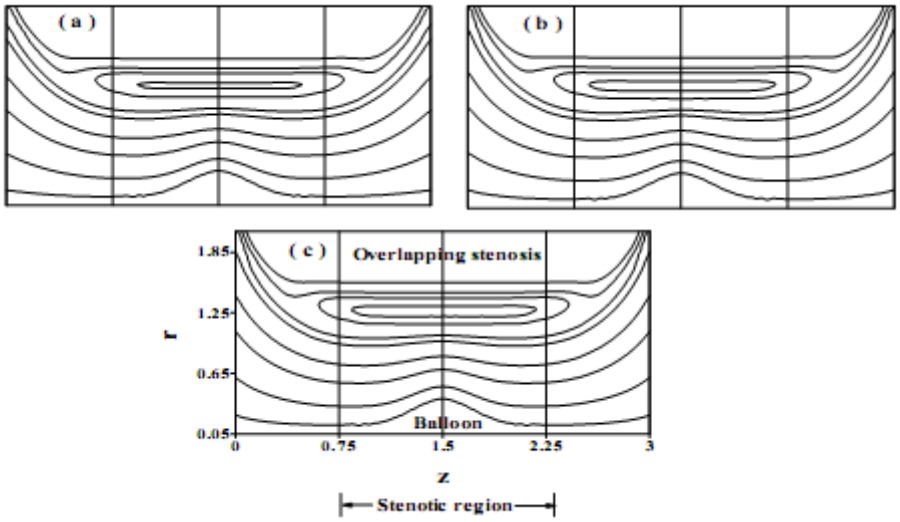

Figure 15 Streamlines for different values of the angle of inclination with (a) $\alpha = 0^o$, (b) $\alpha = 45^o$ and (c) $\alpha = 90^o$.

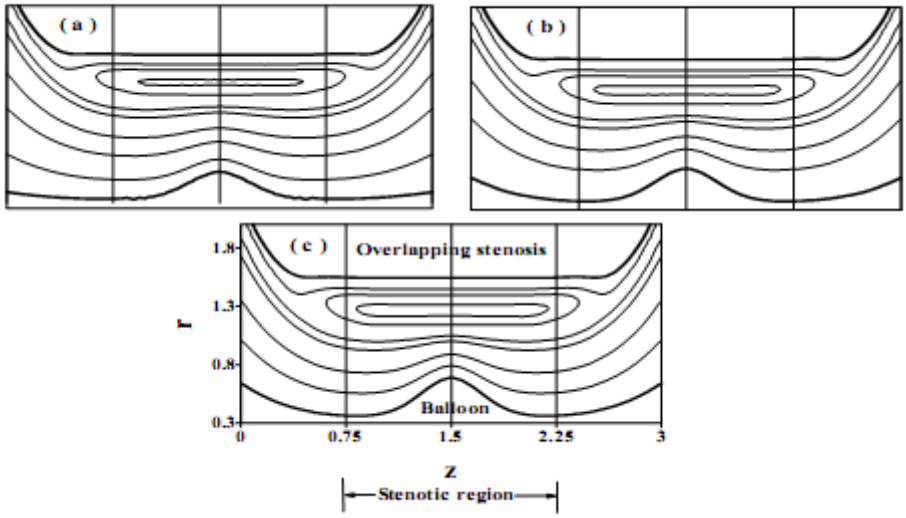

Figure 16 Streamlines for different values of the Weissenberg number with (a) W_i = 0, (b) W_i = 0.01 and (c) W_i = 0.02.

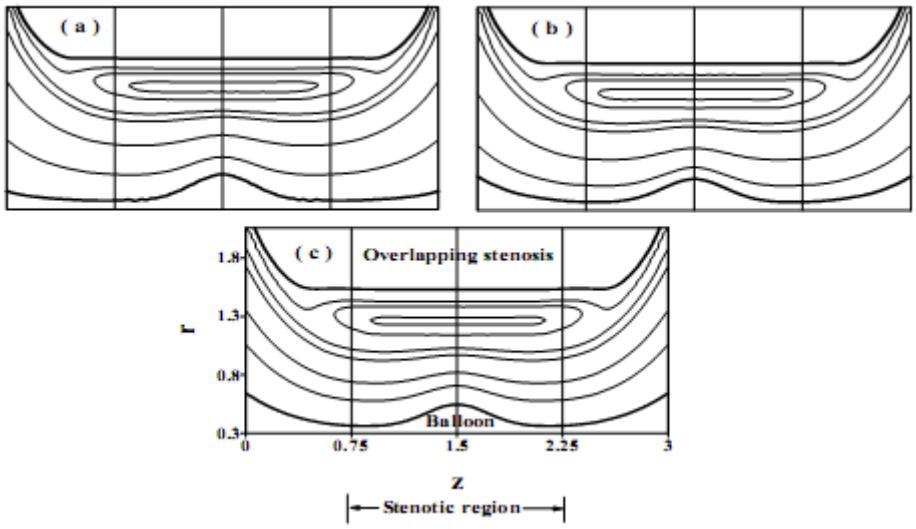

Figure 17 Plot showing streamlines for different values of the power low index with (a) n = 0.398, (b) n = 0.496 and (c) n = 1.

Concluding remarks

The effect of a catheter with a balloon (angioplasty) on the flow of a Carreau fluid (as a blood model) through inclined arteries with time-variant overlapped stenosis is studied. Graphical results are presented for the wall shear stress distributions and resistance to flow (resistance impedance), axial velocity and trapping.

The main finding can be summarized as follows:

1) The transmission of the axial velocity curves through a Newtonian fluid ($W_i = 0, n = 1$) is substantially lower than that for a Carreau fluid in the region near to the wall of the balloon while the inverse occurs in the region between the balloon and stenosis.

2) In the region near to the wall of the balloon the magnitude of axial velocity increase clearly by increasing the acceleration due to gravity and the curves through the vertical tube $(\alpha = 90^o)$ are higher than those in the inclined and horizontal tube $(\alpha = 0^o)$, while the inverse occurs in the region between the balloon and stenosis.

3) The effect of the gravity on the axial velocity and the resistance impedance is negligibly small by increasing the values of the Froud number gradually.

4) Under stenotic conditions, the curves of the axial velocity and resistance impedance through the converging tapered artery are higher than those in the non-tapered artery and the diverging tapered artery while those of the wall shear stress have an inverse behavior.

5) The resistance impedance profiles with time have an oscillation form through tapered overlapped stenosis arteries and this oscillation decays with time.

6) The streamlines have a clearly distinguished shifting toward the stenotic region and this shifting appears near the wall of the balloon, while it disappeared near the stenotic wall.

7) The size of the trapped bolus through the vertical tube $(\alpha = 90^o)$ is higher than those in the inclined and the horizontal tube $(\alpha = 0^o)$.

8) The size of the trapped bolus in the case of a Newtonian fluid ($W_i = 0, n = 1$) is smaller than that through a Carreau fluid.

References

[1] Kh Mekheimer and MA Elkot. The micropolar fluid model for blood flow through stenotic arteries. *Int. J. Pure Appl. Math*. 2007; **4**, 393-405.
[2] Kh Mekheimer and MA Elkot. Influence of magnetic field and Hall currents on blood flow through stenotic artery. *Appl. Math. Mech. Eng. Ed*. 2008; **29**, 1093-104.
[3] Kh Mekheimer and MA Elkot. The micropolar fluid model for blood flow through a tapered arteries with a stenosis. *Acta Mech. Sin*. 2008; **24**, 637-44.
[4] Kh Mekheimer and MA Elkot. Suspension model for blood flow through arterial catheterization. *Chem. Eng. Comm*. 2010; **197**, 1-20.
[5] Kh Mekheimer, MH Haroun and MA Elkot. Effects of magnetic field, porosity, and wall properties for anisotropically elastic multi-stenosis arteries on blood flow characteristics. *Appl. Math. Mech. Eng. Ed.* 2011; **32**, 1047-64.
[6] S Chakravarty and PK Mandal. A nonlinear two-dimensional model of blood flow in an overlapping arterial stenosis subjected to body acceleration. *Math. Comput. Model*. 1996; **24**, 43-58.
[7] S Chakravarty and PK Mandal. Two-dimensional blood flow through tapered arteries under stenotic conditions. *Int. J. Nonlinear Mech.* 2000; **35**, 779-93.
[8] Z Ismail, I Abdullah, N Mustapha and N Amin. Power-law model of blood flow through a tapered overlapping stenosed artery. *Appl. Math. Comput*. 2008; **195**, 669-80.
[9] GC Layek, S Mukhopadhyay and RSD Gorla. Unsteady viscous flow with variable viscosity in a vascular tube with an overlapping constriction. *Int. J. Eng. Sci*. 2009; **47**, 649-59.

[10] VP Srivastava and R Rastogi. Blood flow through stenosed catheterized artery: Effects of hematocrit and stenosis shape. *Comput. Math. Appl*. 2010; **59**, 1377-785.
[11] G Varshney, VK Katiyar and S Kumar. Effect of magnetic field on the blood flow in artery having multiple stenosis: A numerical study. *Int. J. Eng. Sci. Tech.* 2010; **2**, 67-82.
[12] Kh Mekheimer, MH Haroun and MA Elkot. Induced magnetic field influences on blood flow through an anisotropically tapered elastic arteries with overlapping stenosis in an annulus. *Can. J. Phys*. 2011; **89**, 201-12.
[13] T Hayat, S Najma, Y Abdelmaboud and S Asghar. Peristaltic flow of a second-order fluid in the presence of an induced magnetic field. *Int. J. Numer. Meth. Fluid*. 2011; **67**, 537-58.
[14] K Vajravelu, S Sreenadh and VR Babu. Peristaltic transport of a herschel-bulkley fluid in an inclined tube. *Int. J. Nonlinear Mech*. 2005; **40**, 83-90.
[15] KM Prasad and G Radhakrishnamacharya. Flow of herschel-bulkley fluid through an inclined tube of non-uniform cross-section with multiple stenoses. *Arch. Mech*. 2008; **60**, 161-72.
[16] S Nadeem and NS Akbar. Influence of heat transfer on a peristaltic transport of Herschel-Bulkley fluid in a non-uniform inclined tube. *Comm. Nonlinear Sci. Numer Simulat*. 2009; **14**, 4100-13.
[17] S Nadeem and NS Akbar. Peristaltic flow of Walter's B fluid in a uniform inclined tube. *J. Biorheol.* 2010; **24**, 22-8.
[18] KM Prasad, G Radhakrishnamacharya and JV Murthy. Peristaltic pumping of a micropolar fluid in an inclined tube. *Int. J. Appl. Math. Mech*. 2010; **6**, 26-40.
[19] US Chakraborty. Devajyoti biswas and Moumita Paul, suspension model blood flow through an inclined tube with an axially non-symmetrical stenosis. *Korea Aust. Rheol. J.* 2011; **23**, 25-32.
[20] M Khan, Q Abbas and K Duru. Magnetohydrodynamic flow of a Sisko fluid in annular pipe: A numerical study. *Int. J. Numer. Meth. Fluid*. 2010; **62**, 1169-80.
[21] R Ellahi, R Arshad, S Nadeem and M Ali. Peristalic flow of Carreau fluid in a rectangular duct through a porous medium. *Math. Probl. Eng.* 2012; **2012**, Article ID 329639.
[22] AE Naby, AE Hakeem and AEM Misiery. Effects of an endoscope and generalized Newtonian fluid on peristaltic motion. *Appl. Math. Comput*. 2002; **128**, 19-35.
[23] G Jayaraman and A Sarkar. Nonlinear analysis of arterial blood flow-steady streaming effect. *Nonlinear Anal*. 2005; **63**, 880-90.
[24] PK Mandal. Unsteady analysis of non-Newtonian blood flow through tapered arteries with a stenosis. *Int. J. Nonlinear Mech*. 2005; **40**, 151-64.
[25] RB Bird, RC Armstrong and O Hassager. *Dynamics of Polymeric Liquids: Fluid Mechanics*. Vol I. John Wiley & Sons, New York, 1977, p. 1-672.
[26] RI Tanner. *Engineering Rheology*. Oxford University Press, New York, 1985.
[27] DF Young. Effect of a time dependent stenosis of flow through a tube. *J. Eng. Ind*. 1968; **90**, 248-54.